ISSN: 0067-2904

Effect of an inclined magnetic field on peristaltic flow of Bingham plastic fluid in an inclined symmetric channel with slip conditions

Farah Alaa Adnan*, Ahmad M. Abdul Hadi
Department of Mathematics, College of Science, University of Baghdad, Baghdad, Iraq

Abstract

This paper studies the influence of an inclined magnetic field on peristaltic transport of incompressible Bingham plastic fluid in an inclined symmetric channel with heat transfer and mass transfer. Slip conditions for heat transfer and concentration are employed. The formulation of the problem is presented through, the regular perturbation technique for small Bingham number Bn is used to find the final expression of stream function, the flow rate, heat distribution and concentration distribution. The numerical solution of pressure rise per wave length is obtained through numerical integration because its analytical solution is impossible. Also the trapping phenomenon is analyzed. The effect of the physical parameters of the problem are discussed and illustrated graphically

Keywords: an inclined magnetic field, Bingham plastic fluid, an inclined symmetric channel, slip conditions.

تأثير المجال المغناطيسي المائل على الجريان التمعجي لمائع من النوع بنكهام بلاستك خلال قناة مائلة مع وجود شروط الأنزلاق

فرح علاء عدنان*،احمد مولود عبدالهادي
قسم الرياضيات، كلية العلوم، جامعة بغداد، بغداد، العراق

الخلاصة

في هذه البحث قمنا بدراسة تاثير المجال المغناطيسي المائل على الانتقال التمعجي لمائع غير قابل للأنضغاط من النمط بنكهام في قناة متناظرة مائلة مع معادلة الحرارة ومعادلة التركيز. وقد أخذ بنظر ألاعتبار شرط الانزلاق على معادلة الحرارة ومعادلة التركيز. تمت صياغة المعادلات وتبسيطها بأستخدام فرضية الطول الموجي الطويل وتقريب عدد رينولد الصغير. المعادلات التفاضلية اللاخطية تم حلها تحليليا بطريقة الاهتزاز المنتظم لثابت بنكهام الصغير لايجاد دالة الجريان , معدل الجريان ,توزيع الحرارة وتوزيع التركيز.تم حل ارتفاع الضغط باستخدام تكامل عددي وكذلك تمت دراسة ظاهرة الاستداق من خلال الرسوم. كذلك تم تحليل النتائج وعرض تقييم الصوري لبيان السلوك المعلمات المختلفة المضمنة .

1. Introduction

Peristaltic flow in the presence of slip conditions in comparison to non-slip conditions has an important role in many applications especially in the modern material industry (polymer industry where it is given as a microscopic wall slip), medical application (for example polishing artificial hearts),

*Email:farrah.a_adnan@yahoo.com.

engineering, and the technological process. Its importance inspired many researchers to study the impact of slip conditions on the peristaltic flow problem for Newtonian and non-Newtonian fluids. Hayat et al. [1] analyzed the effect of an inclined magnetic field on peristaltic flow of Williamson fluid in an inclined channel with convective slip condition. Hayat et al. [2] analyzed the effect of slip conditions on peristaltic flow of Powell- Eyring fluid. Adel and Abdualhhadi [3] studied the peristaltic transport of MHD Powell-Eyring fluid through a porous medium in an asymmetric channel with slip condition. Bhatti et al. [4] investigated the simultaneous effect of slip and MHD on the peristaltic blood flow of a Jeffery fluid model in a non- uniform porous channel. Tanveer et al. [5] discussed the influence of an inclined magnetic field on the peristaltic flow of a hyperbolic tangent nonofluid in an inclined channel which has flexible walls. Adnan and Abdualhhadi [6] investigated the effect of a magnetic field on a peristaltic transport of Bingham plastic fluid in a symmetrical channel. Adnan and Abdualhhadi [7] studied the effect of the magnetic field on a peristaltic flow of Bingham plastic fluid. Ahmed and Abdualhhadi [8] investigated the effect of a magnetic field on peristaltic flow of Jeffery fluid through a porous medium in a tapered asymmetric channel.

In this study the effect of an inclined magnetic field on the peristaltic transport of Bingham plastic fluid through an inclined symmetric channel with the slip conditions of heat and concentration will be investigated. The large wave length and small Reynolds number concept are taken into considersion to simplify the problem. The regular perturbation technique for small Bingham number $\mathrm{Bn} < 1$ is used to find the final expression of stream function, heat distribution and concentration distribution. The numerical integration of pressure rise is found by using series solution. Finally the influence of different parameters on velocity axial, pressure gradient, pressure rise, the local shear stress, the temperature distribution, the concentration, and the trapping phenomenon are discussed in details with the use of graphs.

2. The mathematical model of the problem

Assume the peristaltic flow of incompressible Bingham plastic fluid in a two dimension tapered symmetric channel with thickness $(2\mathrm{d})$. Both the magnetic field and the channel are inclined at angles $\emptyset$ and α. The x- axis is taken along the length of the channel and y- axis is the opposite of it [see Figure-1)]. A uniform magnetic field $B = (B_0 \sin\emptyset\,, B_0 \cos\emptyset\,, 0)$ is applied. The flow is generated by sinusoidal waves propagating along the compliant walls of the channel.

The structures of the wall geometry is described as follows

$$Y_1 = H_1(X,\bar{t}) = d_1 + a\ \sin\frac{2\pi}{\lambda}(\bar{X} - c\bar{t})\ \text{ Upper wall} \tag{1}$$

$$Y_2 = H_2(X,\bar{t}) = -[d_1 + a\ \sin\frac{2\pi}{\lambda}(\bar{X} - c\bar{t})]\ \text{ Lower wall} \tag{2}$$

In which Y_1 and Y_2 are the upper and lower wall respectively, a is the wave amplitude, λ is the wave length, c is the wave speed and t is the time.

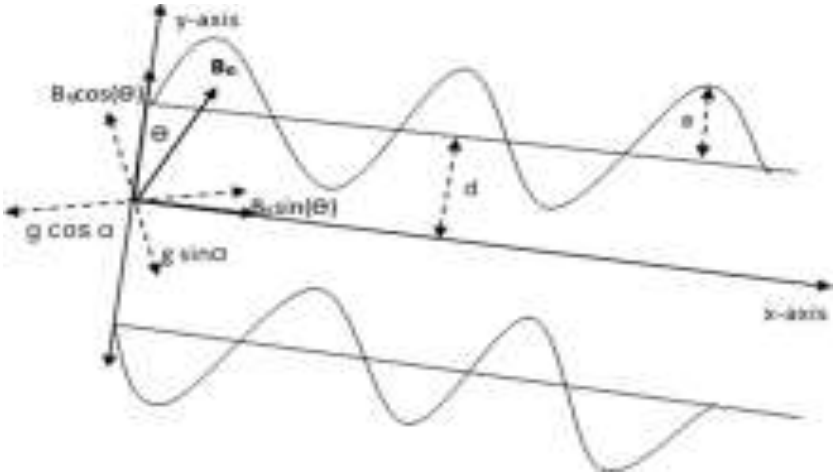

Figure 1-Geometry of the problem

3. The fundamental equation of the problem

The governing equation for the conservation of mass, momentum, energy and concentration for incompressible Bingham plastic fluid in an inclined symmetric channel can be written as follows:

Equation of mass conservation

$$div\ \bar{U} = 0 \tag{3}$$

Equation of momentum in x- direction

$$\rho \frac{d\,\bar{U}}{d\,\bar{t}} = div\ \bar{\tau} - \sigma {B_0}^2\ \cos\emptyset\ (\bar{U}\cos\emptyset - \ \bar{V}\sin\emptyset) + \ \rho g \sin\alpha \tag{4}$$

Equation of momentum in y- direction

$$\rho \frac{d\,\bar{V}}{d\,\bar{t}} = div\ \bar{\tau} + \ \sigma B_0^2 \sin\emptyset\ (\bar{U}\cos\emptyset - \ \bar{V}\sin\emptyset) - \rho g \cos\alpha \tag{5}$$

Equation of energy conservation

$$\rho c_p \frac{d\,\bar{T}}{d\,\bar{t}} = \kappa\nabla^2 T + \bar{S}.(grad\ \bar{U}) + \sigma {B_0}^2(\bar{U}^2\, cos^2\emptyset + \bar{V}^2\, sin^2\emptyset - 2\bar{U}\bar{V}\sin\emptyset\cos\emptyset) + \frac{DK_T}{C_s}\nabla^2 C \tag{6}$$

Equation of particles concentration

$$\frac{dC}{d\bar{t}} = D\nabla^2 C + \frac{DK_T}{T_m}\nabla^2 T \tag{7}$$

Where $\nabla^2 = \frac{\partial^2}{\partial x^2} + \frac{\partial^2}{\partial y^2}$ is the Laplace operator. And $\frac{d}{d\,\bar{t}} = \frac{\partial}{\partial\bar{t}} + \bar{U}\frac{\partial}{\partial\bar{X}} + \bar{V}\frac{\partial}{\partial\bar{Y}}$ is the material time derivative.

Where $(\rho, \sigma, c_p, K_T, D, T_m, g, and\ C_s)$denotes the fluid density, σ is the electrical conductivity, the specific heat, the thermal diffusion ratio, the coefficient of mass diffusivity, the mean temperature, the gravity effect and the concentration susceptibility respectively. Where T is the temperature of the material. The stress tensor for Bingham plastic fluid is described as follows:

$\bar{s} = \left(\mu(\bar{Y}) + \frac{\tau_y}{\dot{\gamma}}\right)\bar{A}_1$, For $\tau \geq \tau_y$,

And the Cauchy stress tensor denoted by $\bar{\tau}$

$\bar{\tau} = -\bar{P}\bar{I} + \bar{S}$, where $\bar{P}$ is the pressure, and $\bar{I}$ the identity tensor then

$$\bar{\tau}_{XX} = -\bar{P} + \bar{S}_{XX}$$
$$\bar{\tau}_{XY} = \bar{S}_{XY}$$
$$\bar{\tau}_{YX} = \bar{S}_{YX}$$
$$\bar{\tau}_{YY} = -\bar{P} + \bar{S}_{YY} \tag{8}$$

Writing the system in laboratory frame, the continuity equation can be written as:

$$\frac{\partial\bar{U}}{\partial\bar{X}} + \frac{\partial\bar{V}}{\partial\bar{Y}} = 0 \tag{9}$$

The $\bar{X}$ and $\bar{Y}$components of the equation of motion are respectively given by

$$\rho\left(\frac{\partial\bar{U}}{\partial\bar{t}} + \bar{U}\frac{\partial\bar{U}}{\partial\bar{X}} + \bar{V}\frac{\partial\bar{U}}{\partial\bar{Y}}\right) = \frac{\partial\bar{\tau}_{XX}}{\partial\bar{X}} + \frac{\partial\bar{\tau}_{XY}}{\partial\bar{Y}} - \ \delta {B_0}^2\ \cos\emptyset\ (\bar{U}\cos\emptyset - \ \bar{V}\sin\emptyset) + \ \rho g \sin\alpha \tag{10}$$

$$\rho\left(\frac{\partial\bar{V}}{\partial\bar{t}} + \bar{U}\frac{\partial\bar{V}}{\partial\bar{X}} + \bar{V}\frac{\partial\bar{V}}{\partial\bar{Y}}\right) = \frac{\partial\bar{\tau}_{XY}}{\partial\bar{X}} + \frac{\partial\bar{\tau}_{YY}}{\partial\bar{Y}} + \ \sigma B_0^2 \sin\emptyset\ (\bar{U}\cos\emptyset - \ \bar{V}\sin\emptyset) - \rho g \cos\alpha \tag{11}$$

The energy equation becomes

$$\rho c_p\left[\frac{\partial\bar{T}}{\partial\bar{t}} + \bar{U}\frac{\partial\bar{T}}{\partial\bar{X}} + \bar{V}\frac{\partial\bar{T}}{\partial\bar{Y}}\right] =$$
$$\kappa\left(\frac{\partial^2\bar{T}}{\partial\bar{X}^2} + \frac{\partial^2\bar{T}}{\partial\bar{Y}^2}\right) + \bar{S}.(grad\ \bar{U}) + \sigma {B_0}^2(\bar{U}^2\, cos^2\emptyset + \bar{V}^2\, sin^2\emptyset - 2\bar{U}\bar{V}\sin\emptyset\cos\emptyset) + \frac{DK_T}{C_s}\left(\frac{\partial^2 C}{\partial\bar{X}^2} + \frac{\partial^2 C}{\partial\bar{Y}^2}\right) \tag{12}$$

The equation of particle s concentration follows as

$$\frac{dC}{d\bar{t}} = D\nabla^2 C + \frac{DK_T}{T_m}\left(\frac{\partial^2 T}{\partial\bar{X}^2} + \frac{\partial^2 T}{\partial\bar{Y}^2}\right) \tag{13}$$

The associated boundary conditions are

$$\bar{U} = 0 \quad at\ \bar{Y} = \bar{H}_1$$
$$\bar{U} = 0 \quad at\ \bar{Y} = \bar{H}_2$$

$$\kappa\frac{\partial T}{\partial \bar{Y}}+\eta_1(T-T_0)=0 \quad at\ \bar{Y}=\bar{H}_1$$
$$\kappa\frac{\partial T}{\partial \bar{Y}}+\eta_1(T_0-T)=0 \quad at\ \bar{Y}=\bar{H}_2$$
$$D\frac{\partial C}{\partial \bar{Y}}+\eta_2(C-C_0)=0 \quad at\ \bar{Y}=\bar{H}_1$$
$$D\frac{\partial C}{\partial \bar{Y}}+\eta_2(C_0-C)=0 \quad at\ \bar{Y}=\bar{H}_2$$
(14)

Applying the mixed condition of heat transfer and mass transfer where η_1 is the heat transfer coefficient and η_2 is the mass transfer coefficient. T_0 is the temperature at the upper wall and C_0 is the concentration at the lower wall.

The flow is time dependent with respect to the laboratory frame $(\bar{X},\bar{Y},\bar{t})$ while in the wave frame with coordinate $(\bar{x},\bar{y})$ moving with the wave speed c the flow is considered steady. Where $\bar{u}$ and $\bar{v}$ are velocity components and $P(\bar{x},\bar{y})$ the pressure in the wave frame. Writing the system equations in a wave frame needs the following transformation between the laboratory frame and wave frame.

$$\bar{x}=\bar{X}-c\bar{t}\ ,\bar{y}=\bar{Y}\ ,\bar{u}=\bar{U}(\bar{X},\bar{Y},\bar{t})-c\ ,\bar{v}=\bar{V}(\bar{X},\bar{Y},\bar{t})$$
$$P(\bar{x},\bar{y})=P(\bar{X},\bar{Y},\bar{t})\ ,T(\bar{x},\bar{y})=T(\bar{X},\bar{Y},\bar{t}),C(\bar{x},\bar{y})=C(\bar{X},\bar{Y},\bar{t}) \quad (15)$$

And defining the following dimensionless quantities

$$x=\frac{2\pi\bar{x}}{\lambda},y=\frac{\bar{y}}{d_1}\ ,u=\frac{\bar{u}}{c}\ ,v=\frac{\bar{v}}{c}\ ,p=\frac{2\pi {d_1}^2\bar{P}}{c\mu_0\lambda}\ ,h_1=\frac{\bar{h}_1}{d_1}\ ,h_2=\frac{\bar{h}_2}{d_1},\ t=\frac{2\pi c\bar{t}}{\lambda},\ \delta=\frac{2\pi d_1}{\lambda}\ ,\ Re=\frac{\rho c d_1}{\mu_0}\ ,$$
$$\dot{\gamma}=\bar{\dot{\gamma}}\frac{\rho d^2}{\mu_0}\ ,\quad s=\frac{d_1}{\mu_0 c}\bar{s}\ ,\ M^2=\frac{\sigma {B_0}^2 {d_1}^2}{\mu_0},\ Pr=\frac{\mu_0 c_p}{k}\ ,Ec=\frac{c^2}{T_0 c_p}\ ,Br=PrEc,\theta=\frac{T-T_0}{T_0}\ ,\ Bn=$$
$$\frac{\tau_y d_1}{\mu_0 c}\ ,\Phi=\frac{C-C_0}{C_1-C_0}\ ,Sc=\frac{\upsilon}{D}\ ,Sr=\frac{DK_T T_0}{\upsilon T_m(C_1-C_0)}\ ,D_u=\frac{DK_T T_0(C_1-C_0)}{\mu_0 c_p\ C_p\ T_0},Fr=\frac{c^2}{g d_1}$$
(16)

Where p is the pressure, $(h_1,\ h_2)$ are channel walls, δ is the wave number, Re is the Reynolds number, M is the Hartman number, Pr is the Prandtl number, Ec is the Eckert number, Br is the Brinkman number, θ is the temperature, Bn is the Bingham number, Sc is the Schmidt number, Sr is the Soret number, and D_u is the Dufour number.

Making use of the above mentioned dimensionless parameter, the channel walls, the continuity equation, motion equations, energy equation and concentration equation and by using the stream function [If $\psi(x,y,t)$ is the stream function, the velocity components in terms of stream function are: $u=\frac{\partial\psi}{\partial y}\ ,v=-\delta\frac{\partial\psi}{\partial x}$] then the resulting system will be reduced as follows:

$$h_1=1+\epsilon\ sinx$$
$$\mathrm{h}_2=-1-\epsilon\ sinx \quad (17)$$

In which $\epsilon=\frac{a}{\mathrm{d}_1}$ is called the geometric parameter (amplitude ratio)

$$\delta\frac{\partial u}{\partial x}+\frac{\partial v}{\partial y}=0 \quad (18)$$

$$\delta\ Re\left(\frac{\partial\psi}{\partial y}+1\right)\frac{\partial u}{\partial x}-Re\ \delta\frac{\partial\psi}{\partial x}\ \frac{\partial}{\partial y}\frac{\partial\psi}{\partial y}=-\frac{\partial p}{\partial x}+\delta\frac{\partial \mathrm{S_{XX}}}{\partial x}+\frac{\partial \mathrm{S_{XY}}}{\partial y}-\ M^2\ \cos\emptyset\left(\left(\frac{\partial\psi}{\partial y}+1\right)\cos\emptyset+\delta\frac{\partial\psi}{\partial x}\sin\emptyset\right)+$$
$$\frac{Re}{Fr}\sin\alpha$$
(19)

$$-\delta^3\ Re\left(\frac{\partial\psi}{\partial y}+1\right)\frac{\partial}{\partial x}\frac{\partial\psi}{\partial x}+\delta^3 Re\ \frac{\partial\psi}{\partial x}\frac{\partial}{\partial y}\frac{\partial\psi}{\partial x}\ =\delta^2\frac{\partial S_{xy}}{\partial x}-\frac{\partial p}{\partial y}+\delta\frac{\partial S_{yy}}{\partial y}+\ \ \delta M^2\sin\emptyset\left(\left(\frac{\partial\psi}{\partial y}+1\right)\cos\emptyset+\right.$$
$$\left.\delta\ \frac{\partial\psi}{\partial x}\ \sin\emptyset\right)-\delta\frac{Re}{Fr}\cos\alpha \quad (20)$$

$$\text{Re Pr}\left[\delta\left(\frac{\partial\psi}{\partial y}+1\right)\frac{\partial\theta}{\partial x}-\delta\frac{\partial\psi}{\partial x}\frac{\partial\theta}{\partial y}\right]=\left(\delta^2\frac{\partial^2\theta}{\partial x^2}+\frac{\partial^2\theta}{\partial y^2}\right)+Br\delta\left(s_{xx}-s_{yy}\right)\frac{\partial}{\partial x}\left(\frac{\partial\psi}{\partial y}\right)+Br\left(\frac{\partial}{\partial y}\left(\frac{\partial\psi}{\partial y}\right)-\delta^2\frac{\partial}{\partial x}\left(\frac{\partial\psi}{\partial x}\right)\right)s_{xy}+Ec\,BrM^2(\left(\frac{\partial\psi}{\partial y}+1\right)^2cos^2\emptyset+(-\delta\frac{\partial\psi}{\partial x})^2sin^2\emptyset+2\left(\frac{\partial\psi}{\partial y}+1\right)\delta\frac{\partial\psi}{\partial x}\sin\emptyset\cos\emptyset)+Du\,Pr(\delta^2\frac{\partial^2\Phi}{\partial x^2}+\frac{\partial^2\Phi}{\partial y^2}) \quad (21)$$

Where $s_{xy}=\mu(y)\left(\frac{\partial^2\psi}{\partial y^2}\right)+B_n$ and B_n is called Bingham fluid number.

$$Re(\delta\left(\frac{\partial\psi}{\partial y}+1\right)\frac{\partial\Phi}{\partial x}-\delta\frac{\partial\psi}{\partial x}\frac{\partial\Phi}{\partial y})=\frac{1}{Sc}(\delta^2\frac{\partial^2\Phi}{\partial x^2}+\frac{\partial^2\Phi}{\partial y^2})+Sr(\delta^2\frac{\partial^2\theta}{\partial x^2}+\frac{\partial^2\theta}{\partial y^2}) \quad (22)$$

Finally the dimensionless of the corresponding boundary condition

$u=-1 \quad at\ y=h_1$
$u=-1 \quad at\ y=h_2$
$\frac{\partial\psi}{\partial x}=-1 \quad at\ y=h_1$
$\frac{\partial\psi}{\partial x}=-1 \quad at\ y=h_2$
$\frac{\partial\theta}{\partial y}+B_{i1}\,\theta=0 \quad at\ y=h_1$
$\frac{\partial\theta}{\partial y}-B_{i1}\theta=0 \quad at\ y=h_2$
$\frac{\partial\Phi}{\partial y}+x_{i1}\Phi=0 \quad at\ y=h_1$
$\frac{\partial\Phi}{\partial y}-x_{i1}\Phi=0 \quad at\ y=h_2$ (23)

Where $B_{i1}=\frac{\eta_1 d_1}{\kappa}$, is the heat transfer Biot number and $x_{i1}=\frac{\eta_2 d_1}{D}$, is the mass transfer Biot number.

Defining$\Theta=F+2$, where Θ is the non-dimensional time mean flow in the fixed frame and F is the non-dimensional time mean flow in the wave frame. And the expression of non-dimensional pressure difference per wave length ΔP_λ is

$$\Delta P_\lambda=\int_0^1\frac{dP}{dx}dx \quad (24)$$

4. Solution to the problem

The resulting system of equations consists of highly nonlinear partial differential equations, because of its hard to find the exact solution. Laminar flow is achieved for a low Reynolds number which produces a free initial term, therefore the solution of this problem is determined by adopting this assumption. The long wave length $\delta\ll 1$ and a low Reynolds number are widely used in the analysis of peristaltic flow. This approximation of a long wave length is based on that the assumption the wave length of the peristaltic wave is larger than the half width of the channel/ tube. Under this assumption neglecting the wave number δ of the equations (19), (20), (21), and (22), the system becomes

$$\frac{\partial p}{\partial x}=\frac{\partial S_{XY}}{\partial y}-M^2\,(\cos\emptyset)^2\left(\left(\frac{\partial\psi}{\partial y}+1\right)\right)+\frac{Re}{Fr}\sin\alpha \quad (25)$$

$$\frac{\partial p}{\partial y}=0 \quad (26)$$

$$\frac{\partial^2\theta}{\partial y^2}+Br\left(\frac{\partial}{\partial y}\left(\frac{\partial\psi}{\partial y}\right)\right)s_{xy}+BrM^2(\left(\frac{\partial\psi}{\partial y}+1\right)^2cos^2\emptyset+Du\,Pr\left(\frac{\partial^2\Phi}{\partial y^2}\right)=0 \quad (27)$$

$$\frac{1}{Sc}\frac{\partial^2\Phi}{\partial y^2}+Sr\frac{\partial^2\theta}{\partial y^2}=0 \quad (28)$$

Assuming the dimensionless quantities, the stream function ψ, the flow rate F, the temperature distribution θ and the concentration distribution Φ will be expended by about the small values of Bingham number Bn.

$\psi=\psi_0+Bn\,\psi_1$
$F=F_0+Bn\,F_1$
$\theta=\theta_0+Bn\,\theta_1$

$$\Phi = \Phi_0 + Bn\,\Phi_1 \quad (29)$$

Putting the above quantities (29) into the equations (25), (27) and (28), then collecting the (terms of like) power of Bn, we obtain the following zeroth and first order systems.

4.1 Zeroth order system

The coefficients of Bn^0 are defined as follows

$$\frac{\partial^4\psi_0}{\partial y^4} = M^2\,(\cos\emptyset)^2\frac{\partial^2\psi_0}{\partial y^2}$$

$$\frac{\partial^2\theta_0}{\partial y^2} + Br\,(\frac{\partial^2\psi}{\partial y^2})^2 + BnBr\frac{\partial^2\psi_0}{\partial y^2} + BrM^2(\frac{\partial\psi_0}{\partial y}+1)^2\,cos^2\emptyset + Du\,Pr\frac{\partial^2\Phi_0}{\partial y^2} = 0$$

$$\frac{1}{Sc}\frac{\partial^2\Phi_0}{\partial y^2} + Sr\frac{\partial^2\theta_0}{\partial y^2} = 0$$

Associated with the boundary conditions

$$\psi_0 = \frac{F_0}{2}, \frac{\partial\psi_0}{\partial y} = -1\,, \frac{\partial\theta_0}{\partial y} + B_{i1}\theta_0 = 0,\ \frac{\partial\Phi_0}{\partial y} + x_{i1}\Phi_0 = 0 \quad at\ \ y = h_1$$

$$\psi_0 = -\frac{F_0}{2}, \frac{\partial\psi_0}{\partial y} = -1\ \,, \frac{\partial\theta_0}{\partial y} - B_{i1}\theta_0 = 0, \frac{\partial\Phi_0}{\partial y} - x_{i1}\Phi_0 = 0 \quad at\ \ y = \mathrm{h}_2$$

4.2 First order system

The coefficients of Bn^1 are defined as follows

$$\left(\frac{\partial^4\psi_1}{\partial y^4} - y\frac{\partial^4\psi_0}{\partial y^4} - 2\frac{\partial^3\psi_0}{\partial y^3}\right) = M^2\,(\cos\emptyset)^2\frac{\partial^2\psi_1}{\partial y^2}$$

$$\frac{\partial^2\theta_1}{\partial y^2} + 2Br\,\frac{\partial^2\psi_0}{\partial y^2}\frac{\partial^2\psi_1}{\partial y^2} - yBr\left(\frac{\partial^2\psi_0}{\partial y^2}\right)^2 + BnBr\frac{\partial^2\psi_1}{\partial y^2} + 2BrM^2\left(\frac{\partial\psi_0}{\partial y}+1\right)^2\frac{\partial\psi_1}{\partial y}cos^2\emptyset + Du\,Pr\frac{\partial^2\Phi_1}{\partial y^2} = 0$$

$$\frac{1}{Sc}\frac{\partial^2\Phi_1}{\partial y^2} + Sr\frac{\partial^2\theta_1}{\partial y^2} = 0$$

Along with the corresponding boundary conditions

$$\psi_1 = \frac{F_1}{2}, \frac{\partial\psi_1}{\partial y} = 0\,, \frac{\partial\theta_1}{\partial y} + B_{i1}\theta_1 = 0\,, \frac{\partial\Phi_1}{\partial y} + x_{i1}\Phi_1 = 0 \quad at\ \ y = h_1$$

$$\psi_1 = -\frac{F_1}{2}, \frac{\partial\psi_1}{\partial y} = 0\ \,, \frac{\partial\theta_1}{\partial y} - B_{i1}\theta_1 = 0\,, \frac{\partial\Phi_1}{\partial y} - x_{i1}\Phi_1 = 0 \quad at\ \ y = \mathrm{h}_2$$

Solving the above zeroth and first order forms with the corresponding boundary conditions, the final form of the stream function, heat and concentration.

5. Result and Discussion

In this section, the numerical and computational results are illustrated and plotted for the problem of the peristaltic transport of Bingham plastic fluid in an inclined symmetric channel with convective condition. Analytical results are shown by using the regular perturbation technique for small value of Bingham parameter Bn. The analysis for velocity distribution, pressure gradient, pressure rise, the local shear stress, the temperature distribution, the concentration, and the trapping phenomenon for the peristaltic flow of Bingham plastic fluid in an inclined symmetric channel.

5.1 Velocity distribution

The outcomes of the axial velocity in terms of different parameters have been plotted and analyzed in this subsection, and it is clear from these graphs that the velocity profiles attain parabolic in nature except if there are some points of reflection on curves of velocity which versa the situations from the increase or decrease. Figures-(2- 6) show the behavior of axial velocity with variation of inclined angle of magnetic field ϕ, the Hartman number M, amplitude ratio ϵ, the parameter of Bingham fluid Bn, and flow rate.

Figure-2 describes the behavior of axial velocity with an increase of inclined angle of magnetic field ϕ. It shows that the velocity profile decreases at the walls but increases in the central part of the channel. The effect of the Hartman number M and amplitude ratio ϵ are sketched in Figures-(3,4), reduction effect of Hartman number and amplitude ratio for axial velocity is observed as the values of M and ϵ increase in the central part of the channel, this is a result of the Lorentz force which opposes the fluid motion and therefore reduces the velocity profile. The velocity profile upon the parameter of Bingham fluid Bn in Figure-5 shows than an increase in the value of the parameter Bn decreases the velocity profile in the lower part of the channel and increases the velocity profile in the upper part of the channel. Figure-6 is

presented to figure out the behavior of an increase of flow rate on the velocity profile. It shows that the velocity profile decreases at the lower and upper parts of the channel while on the central part of the channel the velocity profile increases.

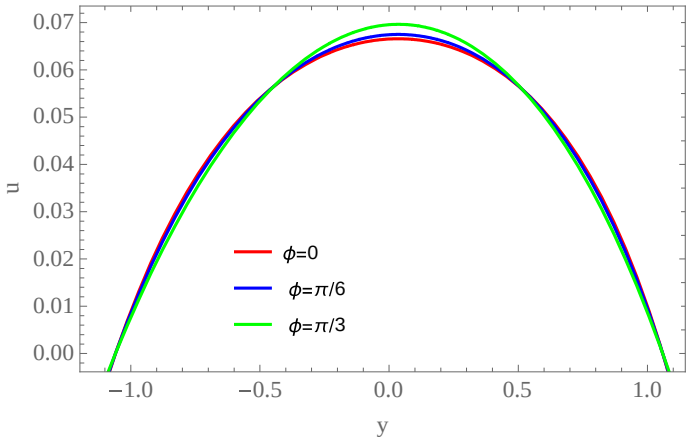

Figure 2- Effect of ϕ on the velocity profile when$M = 2, \mathrm{Bn} = 0.1, \epsilon = 0.2, \mathrm{F0} = 0.1, \mathrm{F1} = 0, \mathrm{x} = 0.3$

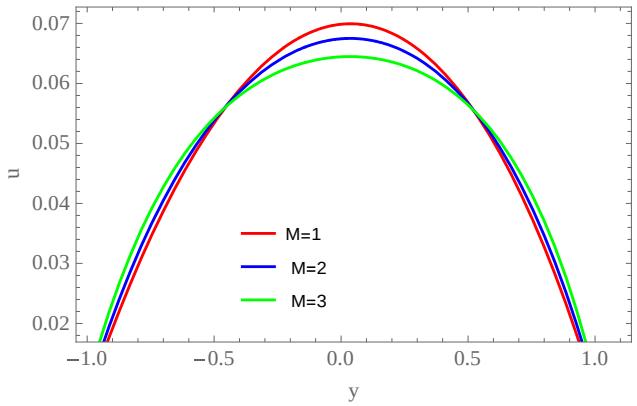

Figure 3- Effect of M on the velocity profile when $\phi = \mathrm{Pi}/6\,, Bn = 0.1, \epsilon = 0.2, \mathrm{F0} = 0.1, \mathrm{F1} = 0, x = 0.3$

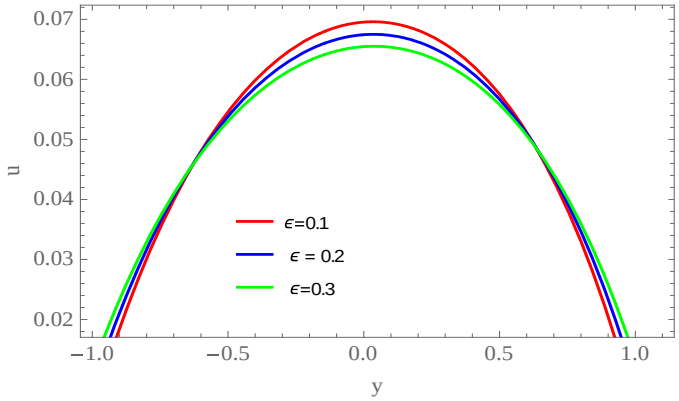

Figure 4- Effect of ϵ on the velocity profile when $\phi = \mathrm{Pi}/6\,, M = 2, Bn = 0.1, \mathrm{F0} = 0.1, \mathrm{F1} = 0, x = 0.3$

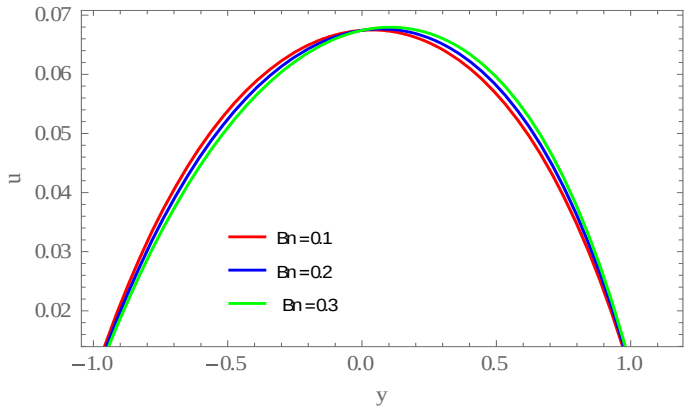

Figure 5- Effect of Bn on the velocity profile when $\phi = \mathrm{Pi}/6, M = 2, \epsilon = 0.2, \mathrm{F0} = 0.1, \mathrm{F1} = 0, x = 0.3$

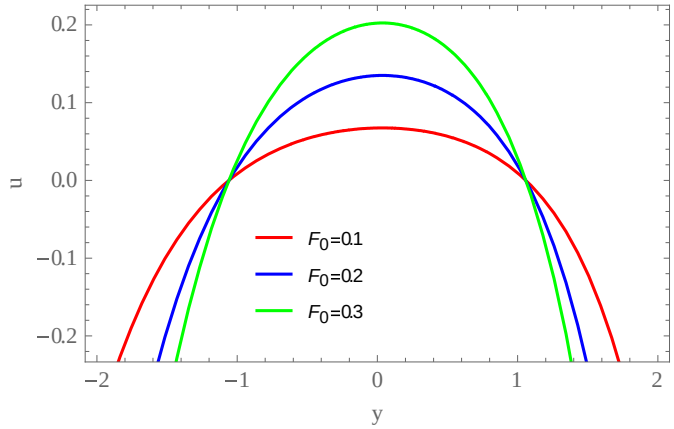

Figure 6- Effect of F0 on the velocity profile when $\phi = \mathrm{Pi}/6, M = 2, Bn = 0.1, \epsilon = 0.2, \mathrm{F1} = 0, x = 0.3$

5.2 Pressure gradient

The physical impact of pertinent parameters on the pressure gradient $\frac{dP}{dx}$ in wave are investigated through Figures-(7-14). The effect of an inclined angle of magnetic field ϕ on the pressure gradient is plotted in Figure-7). It has been seen that for large values of ϕ, the pressure gradient increases. Figure-8 portrays that ascending values of Hartman number M provide a resistance to the flow rate and the pressure gradient decreases. Figure-9 discusses the influence of increasing the Bn pressure gradient. It shows that the pressure gradient decreases with an increase in the Bingham parameter. Figure-10 shows the effect of amplitude ratio ϵ increasing on the pressure gradient, in the vicinity of the channel walls (-$1 \leq x < 0$); $(x > 3.2)$ the magnitude of the pressure gradient decreases but this action reverses in the central part of the channel when the pressure gradient increases. The increase of flow rate on $\frac{dP}{dx}$ is discussed in Figure-11. It is observed that an increase of the flow rate decreases the magnitude of the pressure gradient. Figures-(12, 13) demonstrate the physical reaction of an inclined angle of the channel and Reynolds number on the magnitude of the pressure gradient, an increase in the pressure gradient is noticed upon the increasing of α and Re. Figure-14 shows that an increase of the Froude number decreases the pressure gradient.

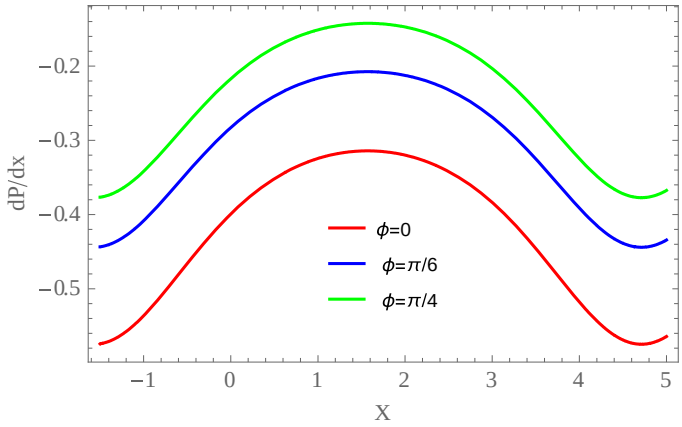

Figure 7- Pressure gradient $\frac{dP}{dx}$ with $M = 0.5, Bn = 0.1, \epsilon = 0.2, \mathrm{F0} = 0.1, \mathrm{F1} = 0, \alpha = \pi/6, \mathrm{Re} = 0.2, \mathrm{fr} = 0.8,$

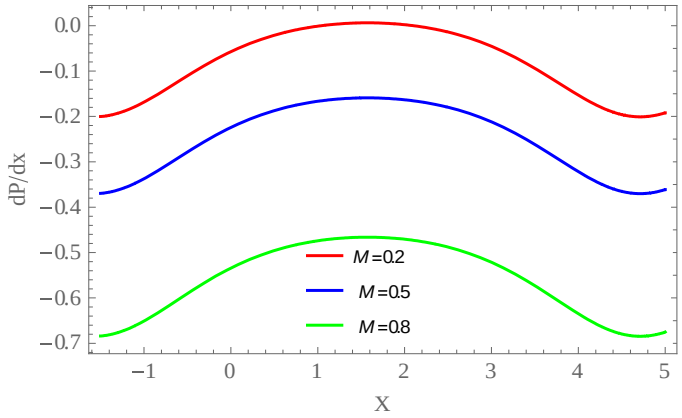

Figure 8- Pressure gradient $\frac{dP}{dx}$ with $\phi = \frac{\pi}{6}, Bn = 0.1, \epsilon = 0.2, \mathrm{F0} = 0.1, \mathrm{F1} = 0, \alpha = \pi/6, \mathrm{Re} = 0.2, \mathrm{fr} = 0.8$

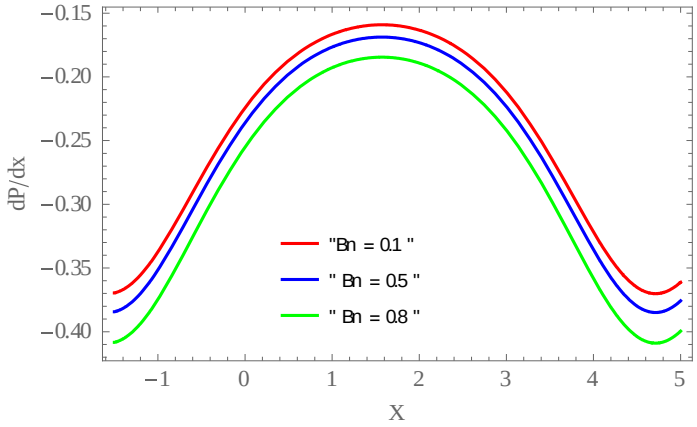

Figure 9- Pressure gradient $\frac{dP}{dx}$ with $\phi = \frac{\pi}{6}, M = 0.5, \epsilon = 0.2, \mathrm{F0} = 0.1, \mathrm{F1} = 0, \alpha = \pi/6, \mathrm{Re} = 0.2, \mathrm{fr} = 0.8$

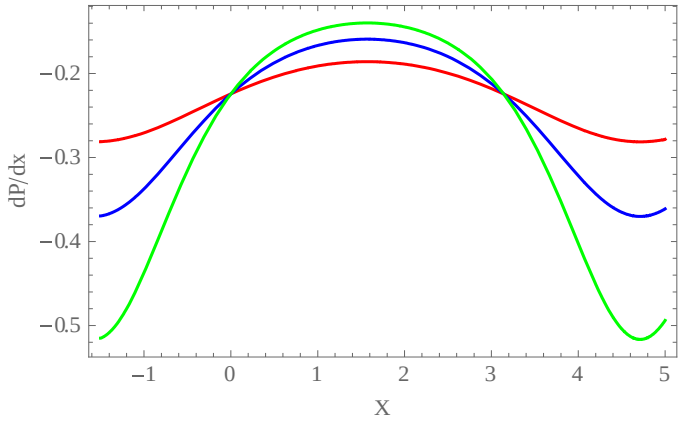

Figure 10- Pressure gradient $\frac{dP}{dx}$ with $\phi = \frac{\pi}{6}, M = 0.5, Bn = 0.1 \mathrm{F0} = 0.1, \mathrm{F1} = 0, \alpha = \pi/6\,, \mathrm{Re} = 0.2, \mathrm{fr} = 0.8$ where $\epsilon = 0.1, \epsilon = 0.2, \epsilon = 0.3$

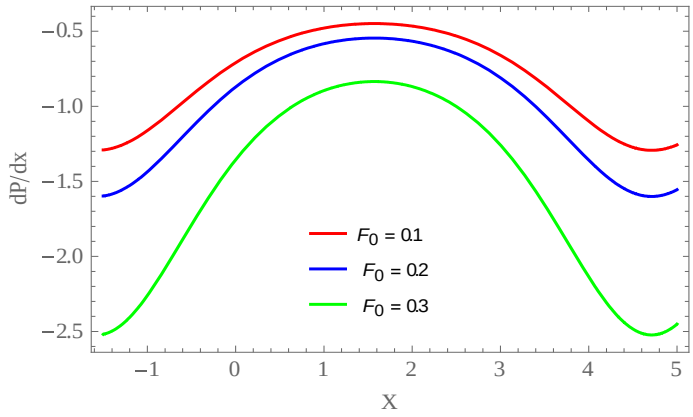

Figure 11- Pressure gradient $\frac{dP}{dx}$ with $\phi = \frac{\pi}{6}, M = 0.5, Bn = 0.1, \epsilon = 0.2, \mathrm{F1} = 0, \alpha = \pi/6\,, \mathrm{Re} = 0.2, \mathrm{fr} = 0.8$

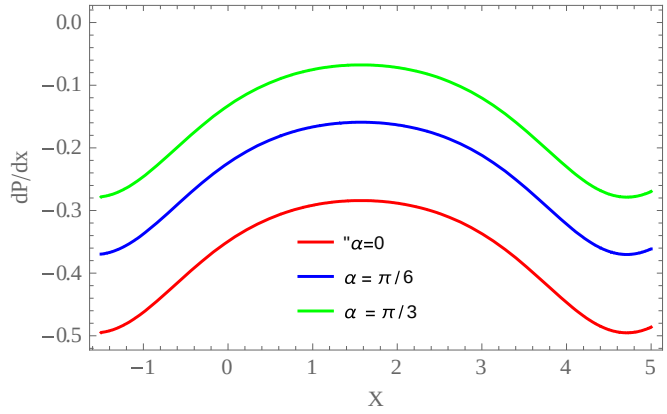

Figure 12- Pressure gradient $\frac{dP}{dx}$ with $\phi = \frac{\pi}{6}, M = 0.5, Bn = 0.1, \epsilon = 0.2, \mathrm{F0} = 0.1, \mathrm{F1} = 0, \mathrm{Re} = 0.2, \mathrm{fr} = 0.8$

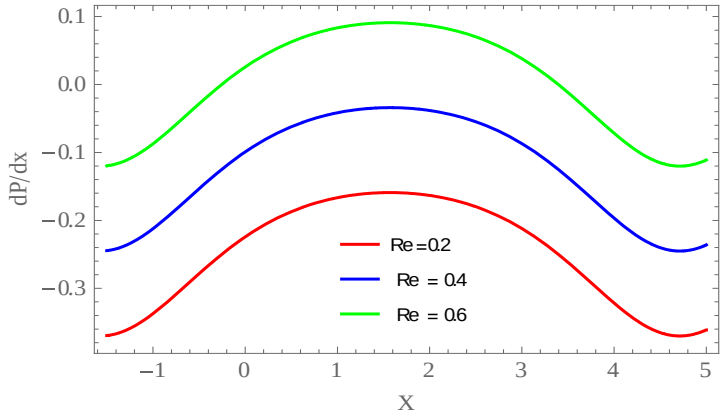

Figure 13- Pressure gradient $\frac{dP}{dx}$ with $\phi = \frac{\pi}{6}, M = 0.5, Bn = 0.1, \epsilon = 0.2, \mathrm{F0} = 0.1, \mathrm{F1} = 0, \alpha = \pi/6, \mathrm{fr} = 0.8$

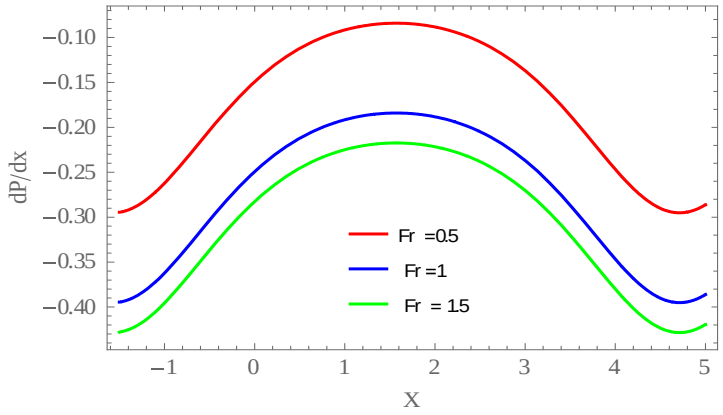

Figure 14- Pressure gradient $\frac{dP}{dx}$ with $\theta = \frac{\pi}{6}, M = 0.5, Bn = 0.1, \epsilon = 0.2, \mathrm{F0} = 0.1, \mathrm{F1} = 0, \alpha = \pi/6, \mathrm{Re} = 0.2$

5.3 Pressure rise

In this subsection, the linear relationship that relates non dimensional average pressure rise per wave length ΔP_λ and dimensionless mean flow rate Θ can be seen in the plots (15)-(21). The influence of various parameters on the pressure rise per wave length ΔP_λ against Θ were investigated. The final expression of ΔP_λ is obtained by numerical integration of series approximation for $\frac{dP}{dx}$ by a Mathematica program. The pumping region is divided in to four regions

1. Retrograde (back word) region where $\Delta P > 0, \Theta < 0$.
2. The co- pumping region where $\Delta P < 0, \Theta < 0$.
3. The augmented region creates for $\Delta P > 0, \Theta > 0$.
4. The free pumping region achieved when $\Delta P = 0$.

Figure-15 illustrates the effect of ϕ on the pumping. It has been seen for large values of ϕ that the pumping rate increase in free pumping and the augmented regions. Figure-16 deduced the pumping via variation of ϵ, it has been noticed that the pumping rate in augmented region and decreases in free pumping and retrograde region. However the opposite results were noticed when the Bingham number increased in Figure-17. It is visualized from Figure-18 that an increase in magnitude of Hartmam number M increases the pumping rate in retrograde region, especially at $\Theta < -2$,and decreases the pumping rate in the augmented region and the free pumping region. Figures-(19, 20) show the effect of an increase of the inclined angle of the channel and the Reynolds number on the pressure rise per wave length ΔP_λ against Θ respectively. It is noticed that the pumping rate increases in the augmented region, free

pumping region and retrograde region. The opposite results were noticed for ascending values of Froude number as is shown in Figure-21

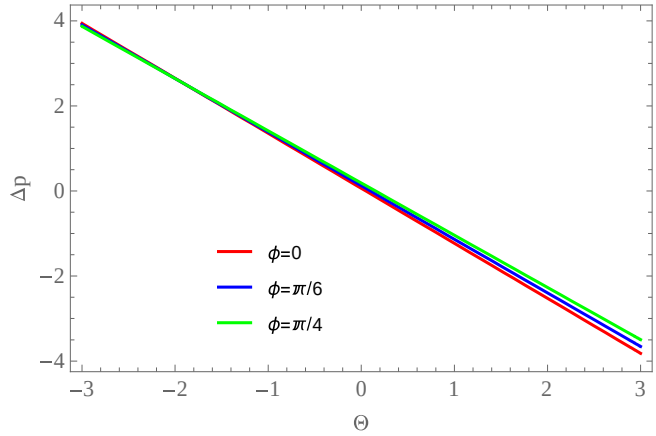

Figure 15- Pressure Rise per wave length with $Bn = 0.5, \epsilon = 0.2, M = 0.5, \alpha = \pi/6, \mathrm{Fr} = 0.8, \mathrm{Re} = 0.5$

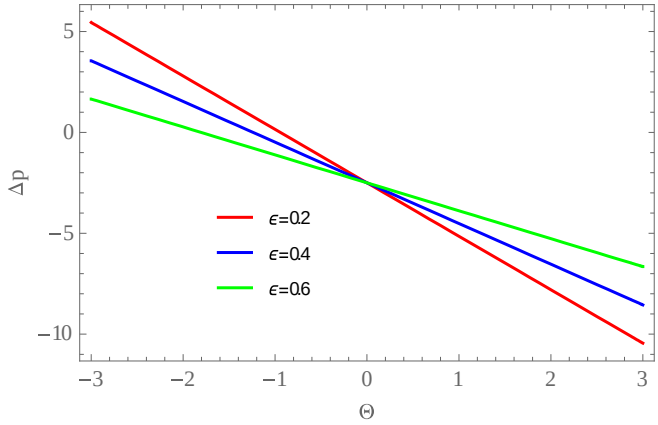

Figure 16- Pressure rise per wave length with $\phi = \pi/6, Bn = 0.5, M = 0.5, \alpha = \pi/6, \mathrm{Fr} = 0.8, \mathrm{Re} = 0.5$

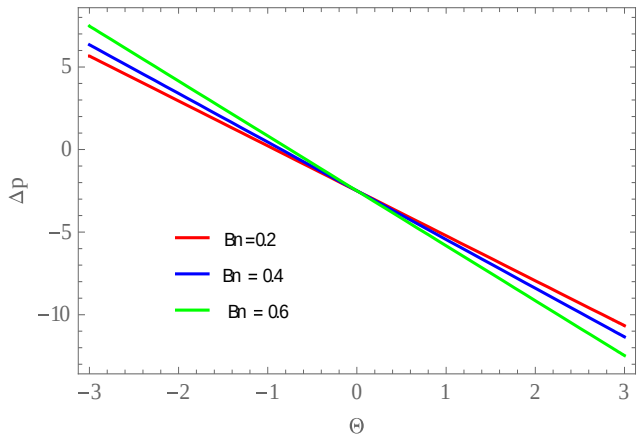

Figure 17- Pressure rise per wave length with $\phi = \pi/6, \epsilon = 0.2, M = 0.5, \alpha = \pi/6, \mathrm{Fr} = 0.8, \mathrm{Re} = 0.5$

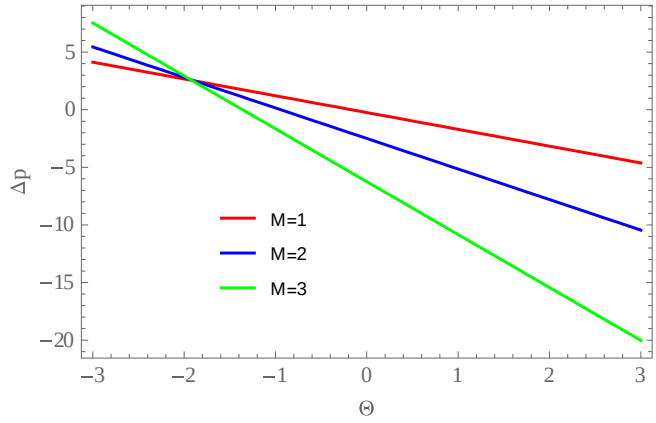

Figure 18- Pressure rise per wave length with $\phi = \pi/6\,, Bn = 0.5, \epsilon = 0.2, \alpha = \pi/6\,, \mathrm{Fr} = 0.8, \mathrm{Re} = 0.5$

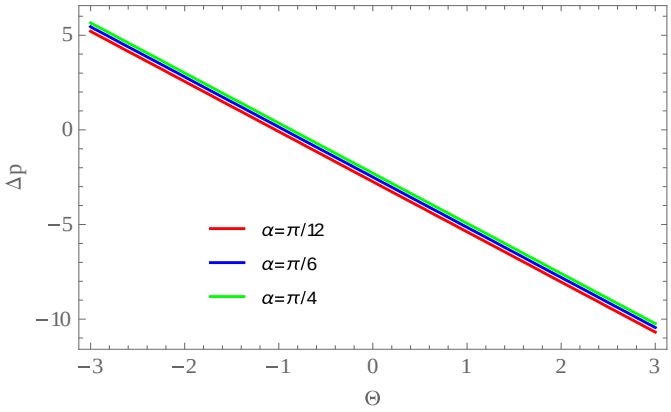

Figure 19- Pressure rise per wave length with $\phi = \pi/6\,, Bn = 0.5, \epsilon = 0.2, M = 0.5, \mathrm{Fr} = 0.8, \mathrm{Re} = 0.5$

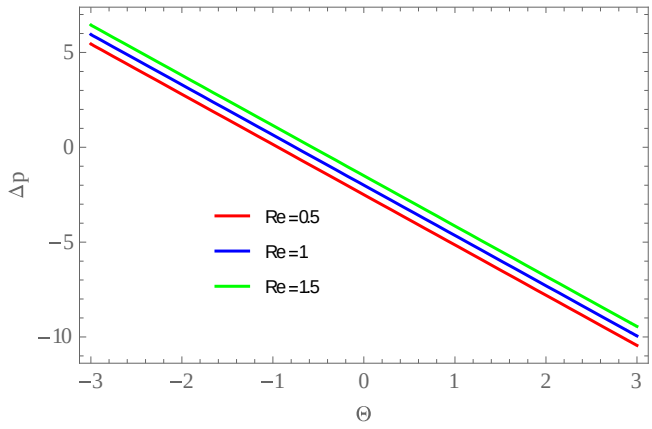

Figure 20- Pressure Rise per wave length with $\phi = \pi/6\,, Bn = 0.5, \epsilon = 0.2, M = 0.5, \alpha = \pi/6\,, \mathrm{Fr} = 0.8$

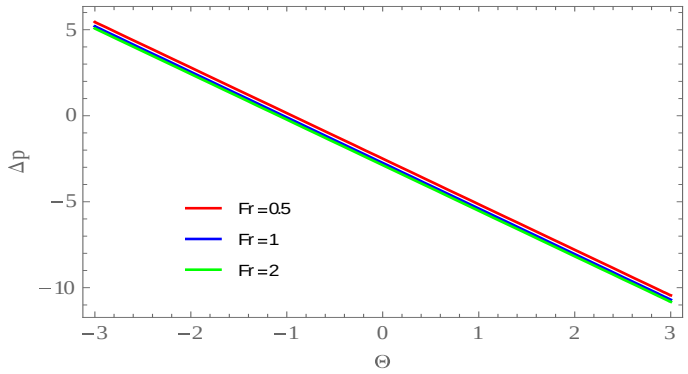

Figure 21- pressure rise per wave length with $\phi = \pi/6\,, Bn = 0.5, \epsilon = 0.2, M = 0.5, \alpha = \pi/6\,,$ Re $=$ 0.5

5.4 Shear stress

The purpose of this subsection is to investigate the effect of various parameters on the local Shear stress equation in the wave frame. The values of shear stress evaluated at a fixed value for $y = 0.1$. Figure-22 detected the impact of increasing the value in ϕ on the S_{xy}. It shows that S_{xy} is a decreasing function. For a large value of Hartman number M and Bingham number Bn the local Shear stress increases through Figure-23, 24. Figure-25 ensures that when the magnitude of amplitude ratio ϵ increases, the value of shear stress decreases at the central part of the channel and increases at the walls of the channel. The impact of the flow rate on the local Shear stress is depicted in Figure-26. It shows that the Shear stress is decreasing in the whole channel and attains its minimal value in the central part of the channel.

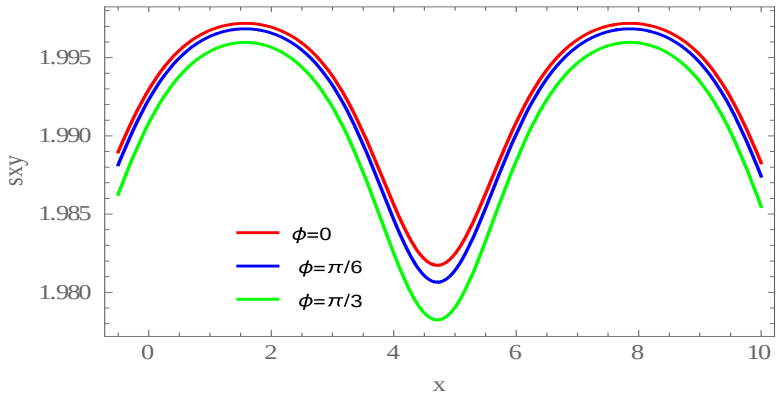

Figure 22- Shear stress with $M = 2, Bn = 0.1, \epsilon = 0.2,$ F0 $= 0.1$

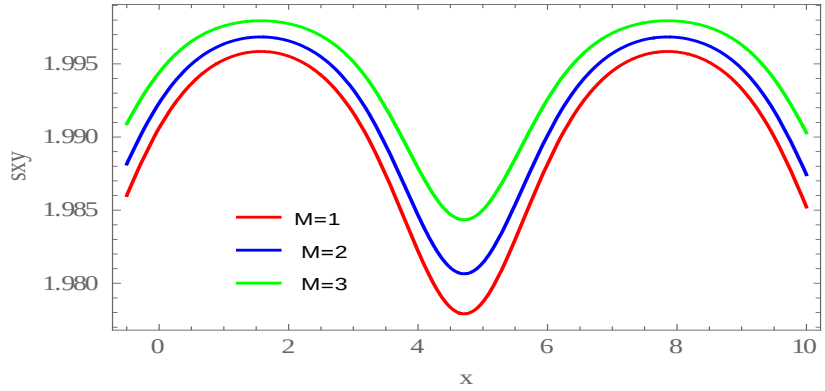

Figure 23- Shear stress with $\phi = \frac{\pi}{6}, Bn = 0.1, \epsilon = 0.2,$ F0 $= 0.1$

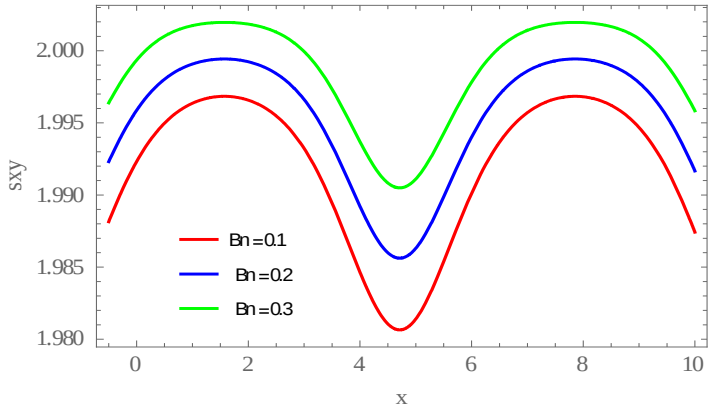

Figure 24- Shear stress with $\phi = \frac{\pi}{6}, M = 2, \epsilon = 0.2, \mathrm{F0} = 0.1$

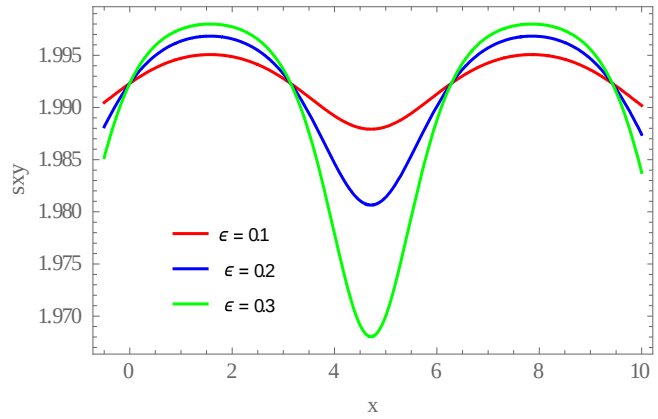

Figure 25- Shear stress with $\phi = \frac{\pi}{6}, M = 2, Bn = 0.1, \mathrm{F0} = 0.1$

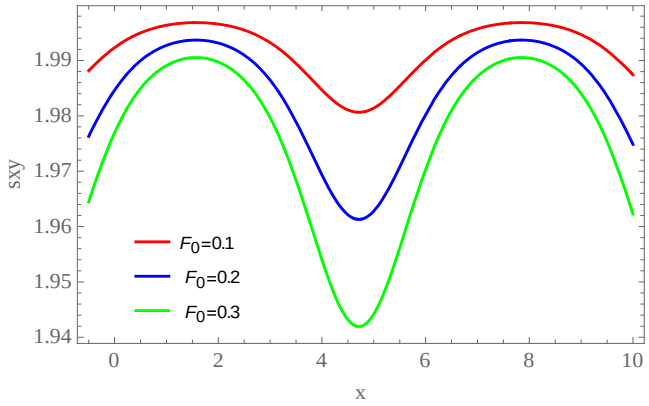

Figure 26- Shear stress with $\phi = \frac{\pi}{6}, M = 2, Bn = 0.1, \epsilon = 0.2$

5.4 Temperature distribution

The effect of different emerging parameters on the temperature distribution $\theta(y)$ are observed physically at a fixed value of $x = 0.3$.through Figures-(27-37). It is observed that throughout all the figures, $\theta(y)$ attains a maximum value near the central part of the channel. Figure-27 shows the effect of ϕ on the temperature profile. It is noted that an increase in the angle ϕ decreases the temperature profile. Figure-28 shows that the temperature profile is an increasing function with an increase of Bingham

number Bn. The variation in temperature with an increase of amplitude ratio ϵ is discussed in Figure-29. It is noted that the temperature profile increases. The influence of the flow rate on the temperature profile increase in Figure-30, where it is noted that there is an increase in the central part of the channel. The temperature profile shows an increased function for higher values of Hartman number M, Dufour number, Soret number, Schmidt number, Prandtl number, and Brinkman number as illustrated in Figures-(31-36). Figure-37 is devoted to explain the influence of variations of B_{i1}, the heat transfer Biot number. It is observed that $\theta(y)$ is decreasing with an increase of B_{i1}.

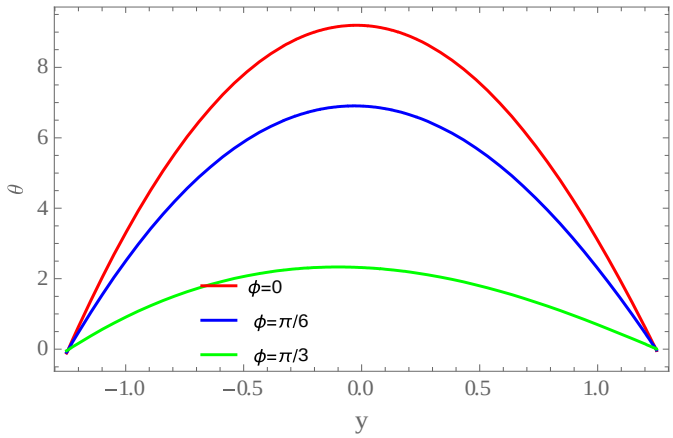

Figure 27- Effect of ϕ on $\theta(y)$when $Bn = 0.1, \epsilon = 0.2, \mathrm{F0} = 0.1, M = 2, \mathrm{Du} = 0.5, \mathrm{Sr} = 0.5, \mathrm{Sc} = 0.5, B_{i1} = 5, \mathrm{Pr} = 2, \mathrm{Br} = 2$

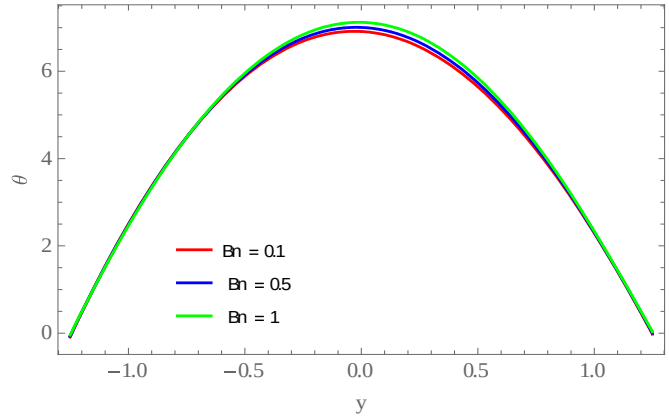

Figure 28- Effect of Bn on $\theta(y)$when $\phi = \pi/6, \epsilon = 0.2, \mathrm{F0} = 0.1, M = 2, \mathrm{Du} = 0.5, \mathrm{Sr} = 0.5, \mathrm{Sc} = 0.5, B_{i1} = 5, \mathrm{Pr} = 2, \mathrm{Br} = 2$

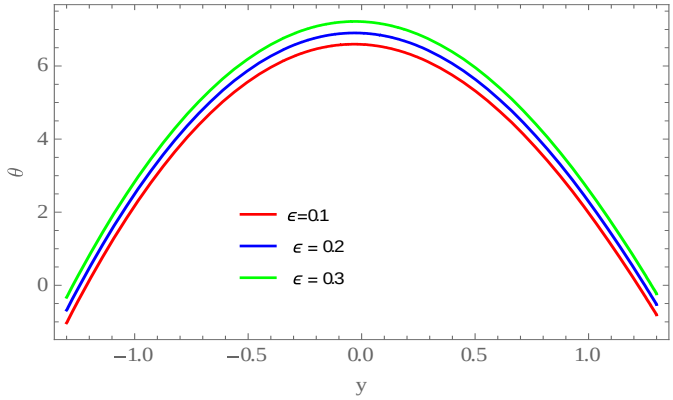

Figure 29- Effect of ϵ on of $\theta(y)$when $\phi = \pi/6, Bn = 0.1, \mathrm{F0} = 0.1, M = 2, \mathrm{Du} = 0.5, \mathrm{Sr} = 0.5, \mathrm{Sc} = 0.5, B_{i1} = 5, \mathrm{Pr} = 2, \mathrm{Br} = 2$

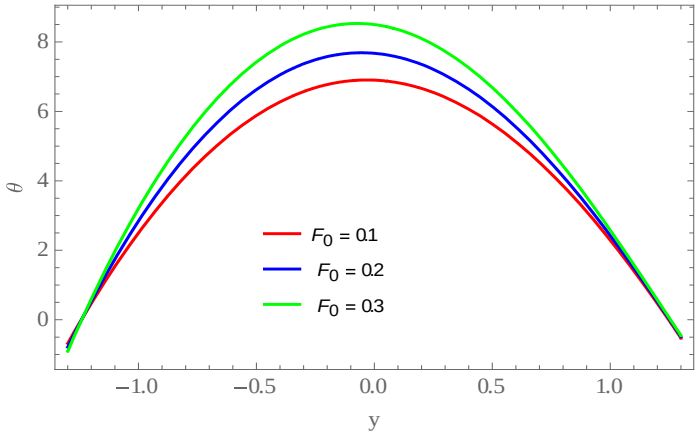

Figure 30- Effect Of F0 on $\theta(y)$when $\phi = \pi/6\,, Bn = 0.1, \epsilon = 0.2, M = 2, \mathrm{Du} = 0.5, \mathrm{Sr} = 0.5, \mathrm{Sc} = 0.5, B_{i1} = 5, \mathrm{Pr} = 2, \mathrm{Br} = 2$

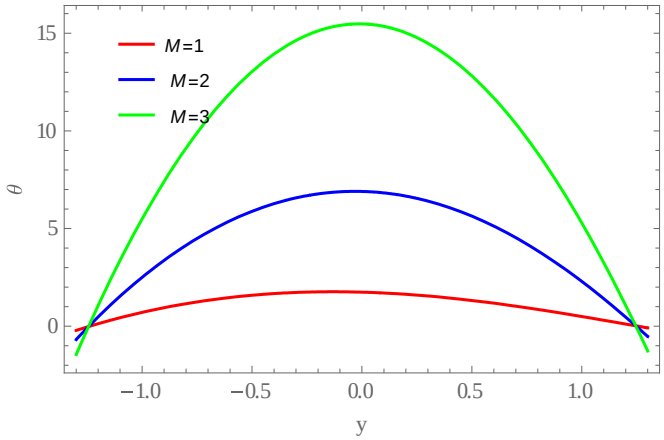

Figure 31- Effect of M on of $\theta(y)$when $\phi = \pi/6\,, Bn = 0.1, \epsilon = 0.2, \mathrm{F0} = 0.1, \mathrm{Du} = 0.5, \mathrm{Sr} = 0.5, \mathrm{Sc} = 0.5, B_{i1} = 5, \mathrm{Pr} = 2, \mathrm{Br} = 2$

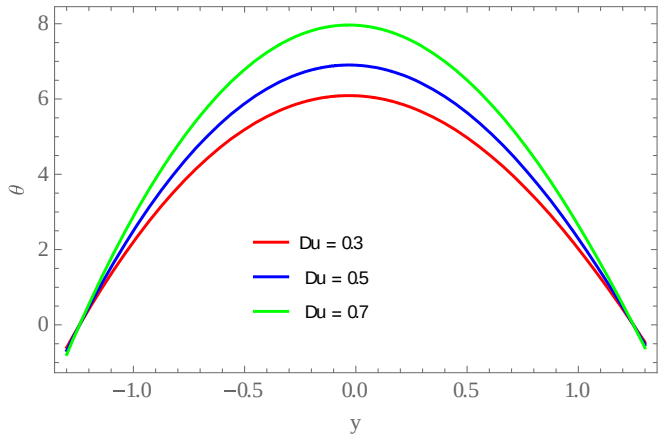

Figure 32- Effect of Du on $\theta(y)$when $\phi = \pi/6\,, Bn = 0.1, \epsilon = 0.2, \mathrm{F0} = 0.1, M = 2, \mathrm{Sr} = 0.5, \mathrm{Sc} = 0.5, B_{i1} = 5, \mathrm{Pr} = 2, \mathrm{Br} = 2$

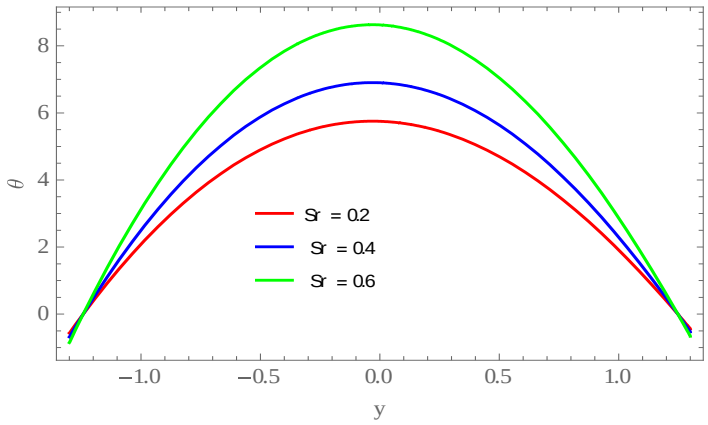

Figure 33- Effect Of Sr on $\theta(y)$when $\phi = \pi/6\,, Bn = 0.1, \epsilon = 0.2, \mathrm{F0} = 0.1, M = 2, \mathrm{Du} = 0.5, \mathrm{Sc} = 0.5, B_{i1} = 5, \mathrm{Pr} = 2, \mathrm{Br} = 2$

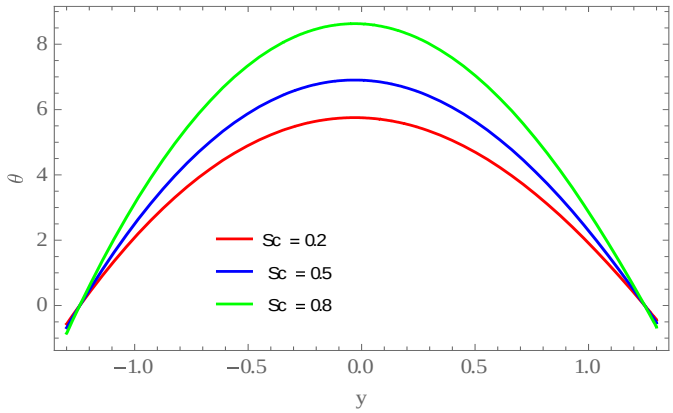

Figure 34- Effect of Sc on $\theta(y)$when $\phi = \pi/6\,, Bn = 0.1, \epsilon = 0.2, \mathrm{F0} = 0.1, M = 2, \mathrm{Du} = 0.5, \mathrm{Sr} = 0.5, B_{i1} = 5, \mathrm{Pr} = 2, \mathrm{Br} = 2$

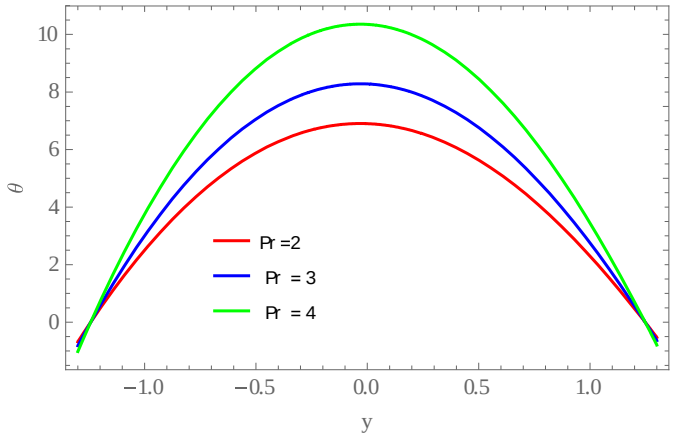

Figure 35- Effect of Pr on $\theta(y)$when $\phi = \pi/6\,, Bn = 0.1, \epsilon = 0.2, \mathrm{F0} = 0.1, M = 2, \mathrm{Du} = 0.5, \mathrm{Sr} = 0.5, \mathrm{Sc} = 0.5, B_{i1} = 5, \mathrm{Br} = 2$

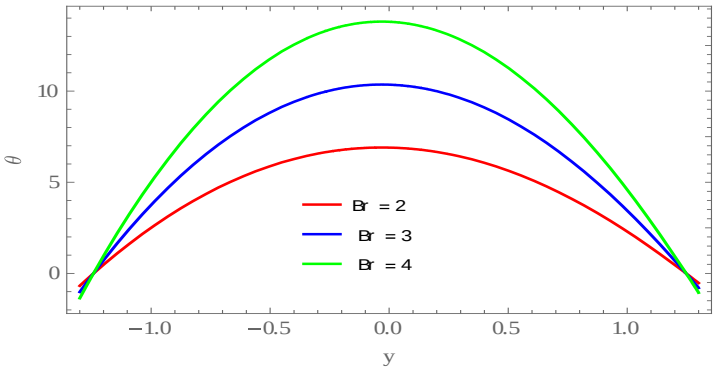

Figure 36- Effect of Br on $\theta(y)$when $\phi = \pi/6\,, Bn = 0.1, \epsilon = 0.2, \mathrm{F0} = 0.1, M = 2, \mathrm{Du} = 0.5, \mathrm{Sr} = 0.5, \mathrm{Sc} = 0.5, B_{i1} = 5, \mathrm{Pr} = 2$

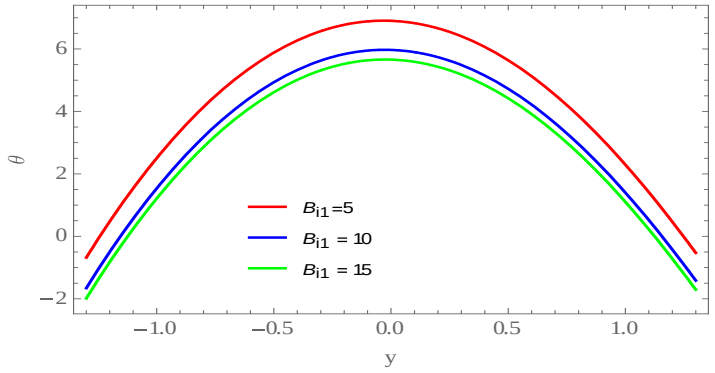

Figure 37- Effect of B_{i1} on **of** $\theta(y)$when $\phi = \pi/6\,, Bn = 0.1, \epsilon = 0.2, \mathrm{F0} = 0.1, M = 2, \mathrm{Du} = 0.5, \mathrm{Sr} = 0.5, \mathrm{Sc} = 0.5, \mathrm{Pr} = 2, \mathrm{Br} = 2$

5.6 Concentration distribution

The concentration of particles for various parameters is checked through Figures-38-47 at a fixed value of $x = 0.3$. The results are a similar trend to the effect of the parameters on the temperature to particles, and being opposite to the effect of parameters on the temperature. Figure-38 shows the impact of increasing the value in ϕ on the concentration profile $\Phi(\mathrm{y})$. It is observed that $\Phi(\mathrm{y})$ increases. Figure-39 illustrates the effect of amplitude ratio ϵ on the concentration profile $\Phi(\mathrm{y})$. It has been seen that for large values of ϵ the concentration profile decreases. It is visualized from Figures-(40-46) that an increase in magnitude of the Hartman number M, the flow rate F_0, the Dufour number Du, the Soret number Sr, the Schmidt number Sc,the Prandtl number and the Pr and the Brinkman number Br increases the concentration profiles $\Phi(\mathrm{y})$. Figure-47 deduced that the concentration profile $\Phi(\mathrm{y})$ increases with an increase of the mass transfer Biot number x_{i1}.

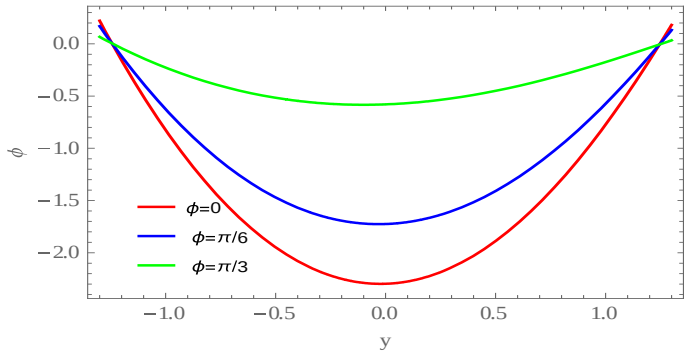

Figure 38- The Effect of ϕ on the $\Phi(\mathrm{y})$ with $Bn = 0.1, \epsilon = 0.2, \mathrm{F0} = 0.1, M = 2, \mathrm{Du} = 0.5, \mathrm{Sr} = 0.5, \mathrm{Sc} = 0.5, x_{i1} = 5, \mathrm{Pr} = 2, \mathrm{Br} = 2$

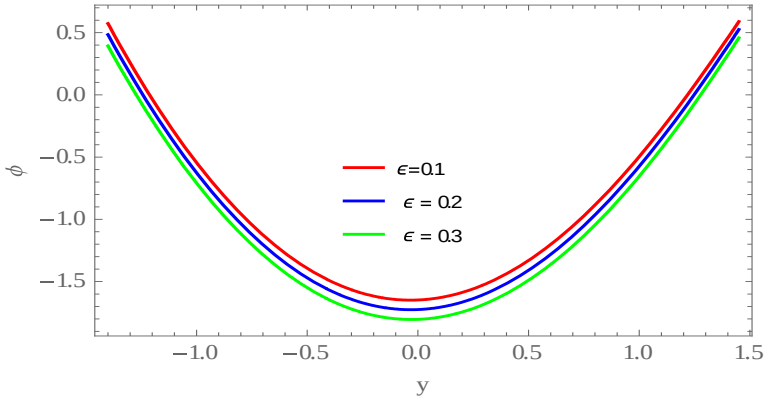

Figure 39- The Effect of ϵ on the $\Phi(y)$ with $\phi = \pi/6, Bn = 0.1, F0 = 0.1, M = 2, Du = 0.5, Sr = 0.5, Sc = 0.5, x_{i1} = 5, Pr = 2, Br = 2.$

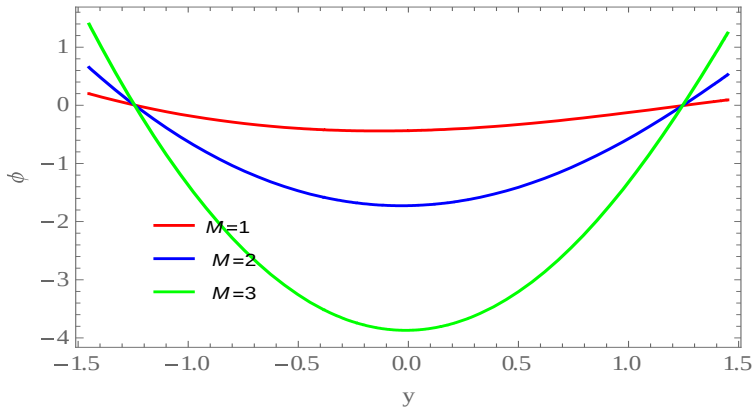

Figure 40- The Effect of M on the $\Phi(y)$ with $\phi = \pi/6, Bn = 0.1, \epsilon = 0.2, F0 = 0.1, Du = 0.5, Sr = 0.5, Sc = 0.5, x_{i1} = 5, Pr = 2, Br = 2$

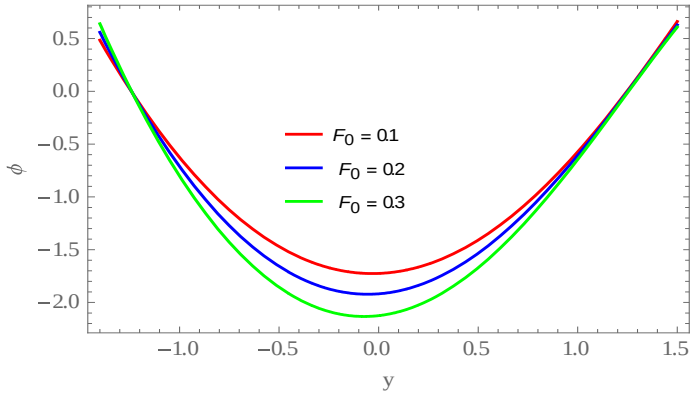

Figure 41- The effect of F0 on the $\Phi(y)$ with $\phi = \pi/6, Bn = 0.1, \epsilon = 0.2, M = 2, Du = 0.5, Sr = 0.5, Sc = 0.5, x_{i1} = 5, Pr = 2, Br = 2$

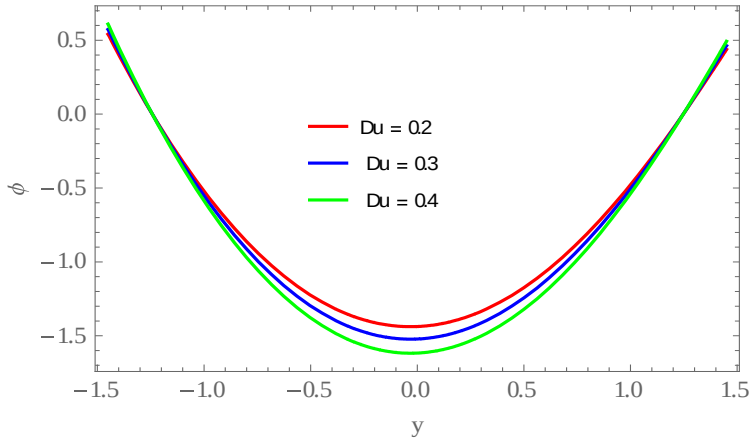

Figure 42- The effect of Du on the $\Phi(y)$ with $\phi = \pi/6, Bn = 0.1, \epsilon = 0.2, F0 = 0.1, M = 2, Sr = 0.5, Sc = 0.5, x_{i1} = 5, Pr = 2, Br = 2$

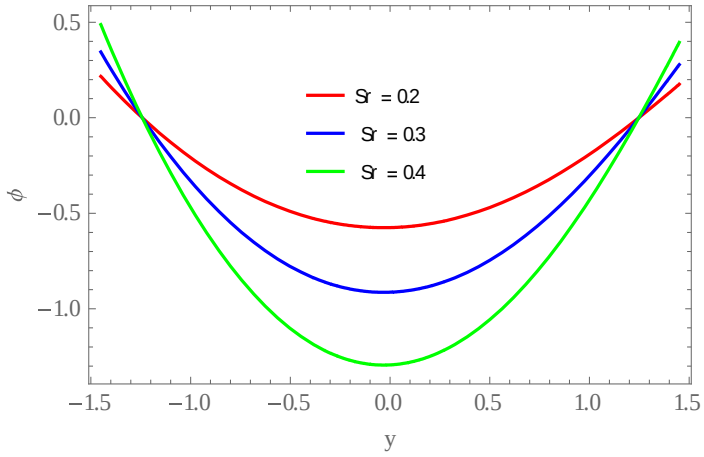

Figure 43- The effect of Sron the $\Phi(y)$ with $\phi = \pi/6, Bn = 0.1, \epsilon = 0.2, F0 = 0.1, M = 2, Du = 0.5, Sc = 0.5, x_{i1} = 5, Pr = 2, Br = 2$

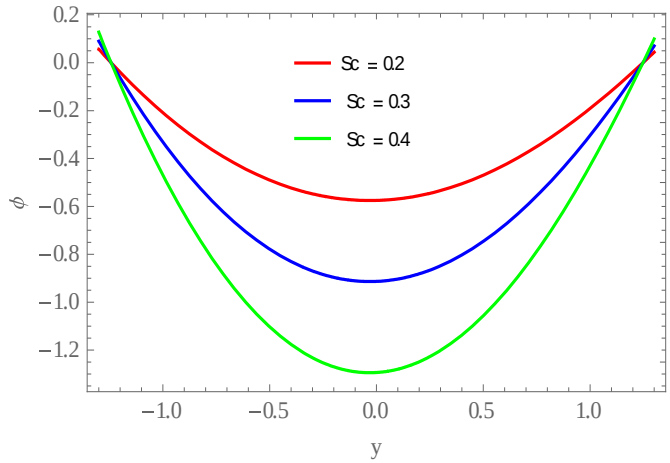

Figure 44- The effect of Sc on the $\Phi(y)$ with $\phi = \pi/6, Bn = 0.1, \epsilon = 0.2, F0 = 0.1, M = 2, Du = 0.5, x_{i1} = 5, Pr = 2, Br = 2$

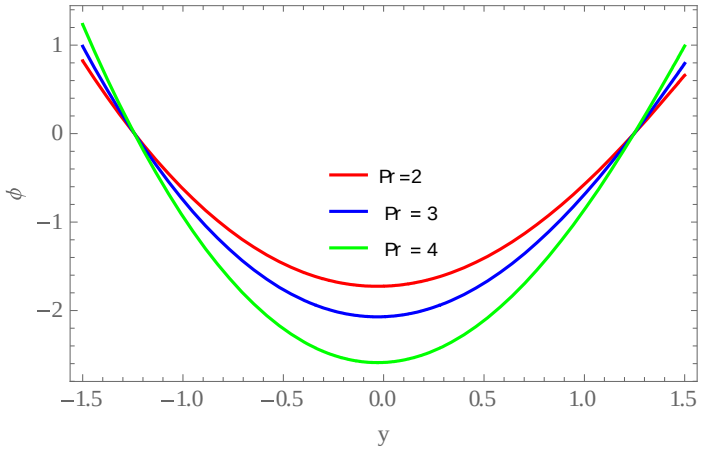

Figure 45- The effect of Pr on the $\Phi(y)$ with $\phi = \pi/6, Bn = 0.1, \epsilon = 0.2, F0 = 0.1, M = 2, Du = 0.5, Sr = 0.5, Sc = 0.5, x_{i1} = 5, Br = 2$

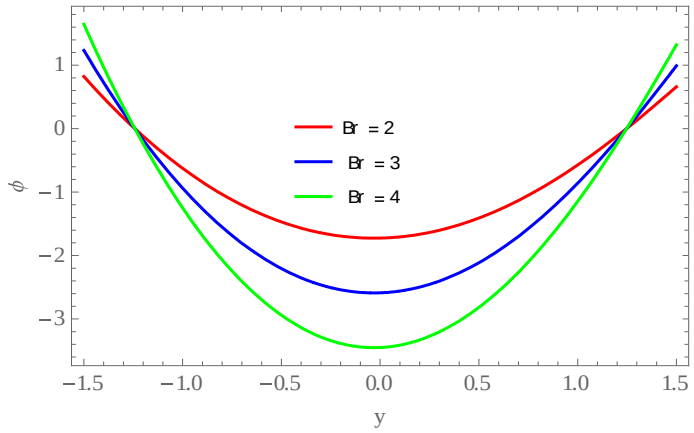

Figure 46- The effect of Br on the $\Phi(y)$ with $\phi = \pi/6, Bn = 0.1, \epsilon = 0.2, F0 = 0.1, M = 2, Du = 0.5, Sr = 0.5, Sc = 0.5, x_{i1} = 5, Pr = 2$

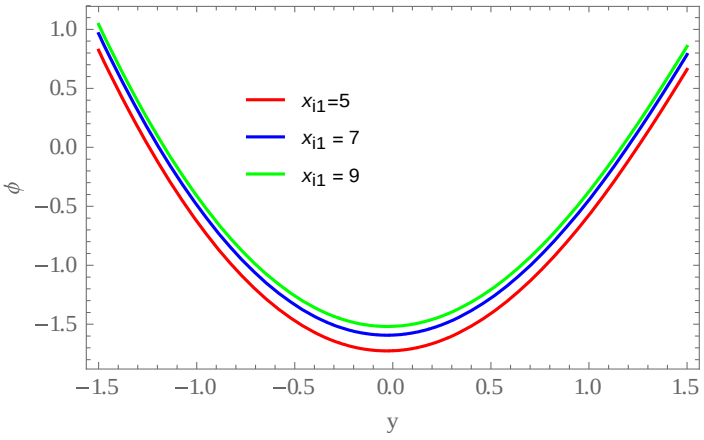

Figure 47- The effect of x_{i1} on the $\Phi(y)$ with $\phi = \pi/6, Bn = 0.1, \epsilon = 0.2, F0 = 0.1, M = 2, Du = 0.5, Sr = 0.5, Sc = 0.5, Pr = 2, Br = 2$

5.7 Trapping

An interesting topic in peristaltic transport is the phenomenon of trapping. The formation of an internally circulating bolus of fluid through closed stream lines is called trapping and this trapped bolus is moving ahead through the peristaltic waves with the same speed as the wave. This phenomenon physically

appears in thrombus in blood and the movement of blood bolus. The trapping for different values of parameters are shown in Figures-(48-51). The stream lines of different values of ϕ is shown in Figure-48. It has been noticed that the size and the number of trapped bolus increased. Figure-49 deduced that for large values of the Hartman number M, the size of the bolus get smaller. Figure-50 display the impact of Bingham number Bn on the stream lines. It is noticed that the number and the size of the bolus decreases for large values of the Bingham number. Figure-51 shows the effect of amplitude ratio ϵ on the stream lines. It is observed that the number and the size of the bolus increases with an increase of ϵ.

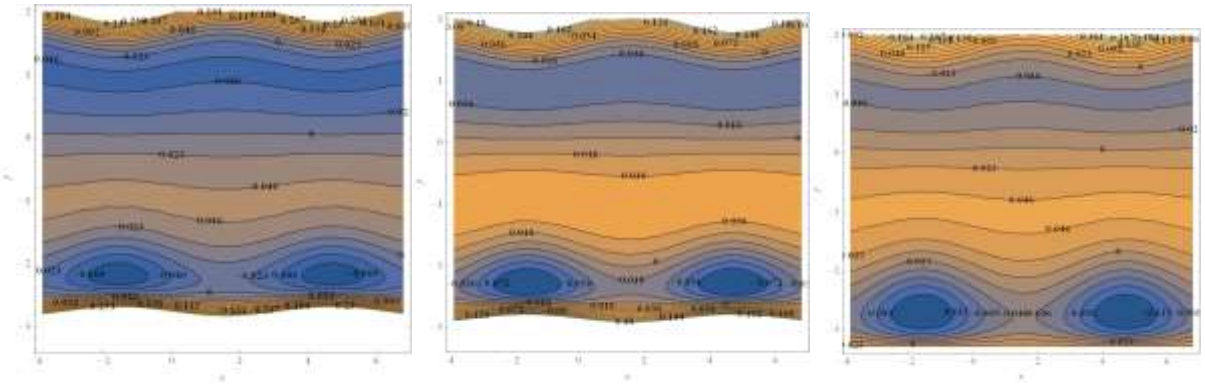

Figure 48-Effect of $[\phi = 0, \phi = \frac{\pi}{6}, \phi = \frac{\pi}{3}]$ on stream lines when $M = 2, Bn = 0.4, \epsilon = 0.1$

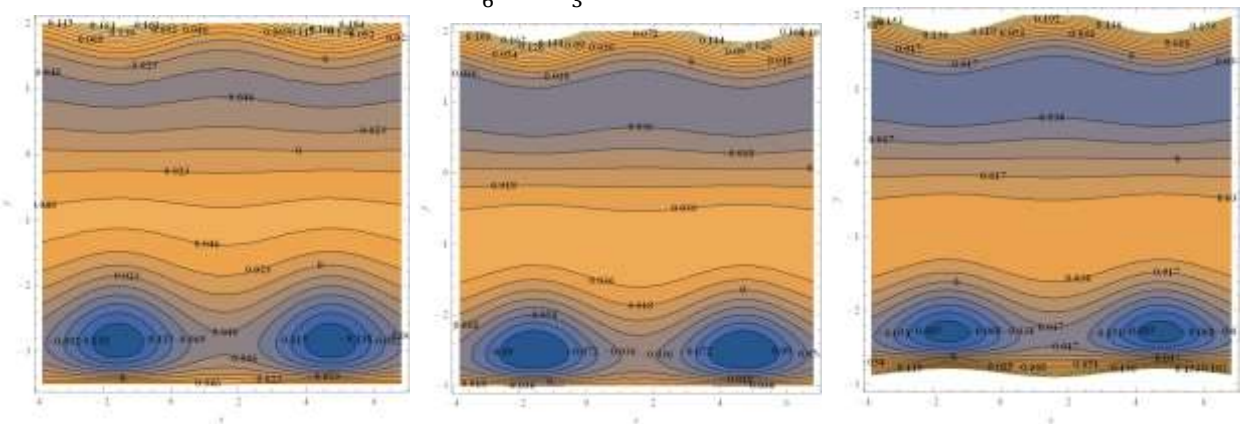

Figure 49-Effect of $[M = 1.5, M = 2, M = 2.5]$ on stream lines when $\phi = \pi/6\,, Bn = 0.4, \epsilon = 0.1$

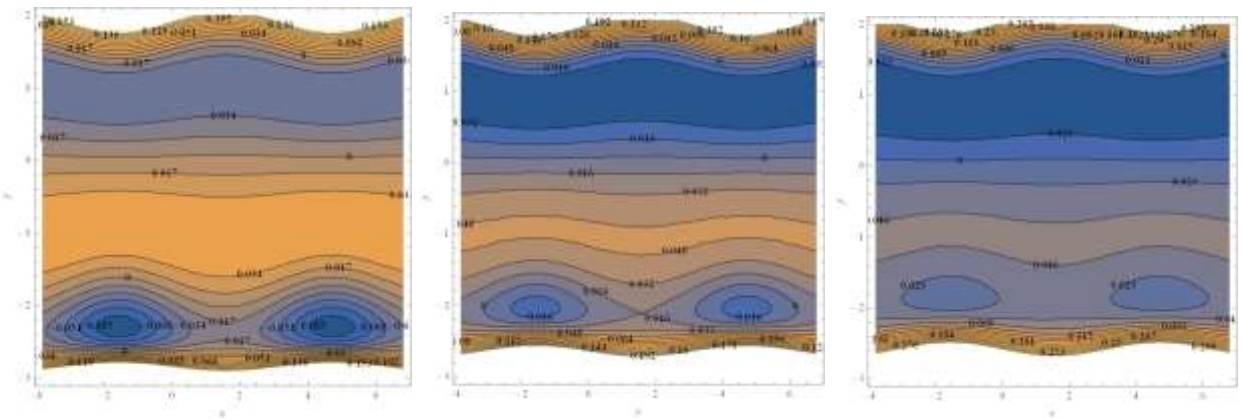

Figure 50-Effect of $[Bn = 0.4, Bn = 0.5, Bn = 0.6]$ on stream lines when $\phi = \pi/6\,, M = 2, \epsilon = 0.1$

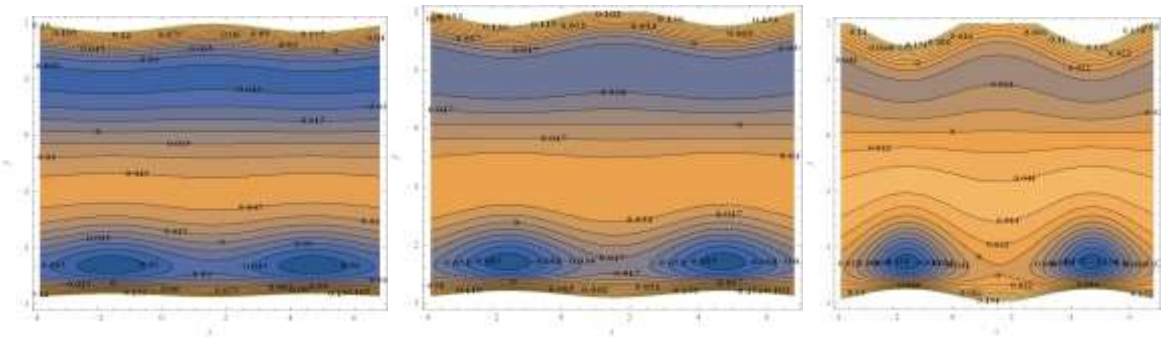

Figure 51-Effect of $[\epsilon = 0.05, \epsilon = 0.1, \epsilon = 0.2]$ on stream lines when $\phi = \pi/6, M = 2, Bn = 0$.

6. Conclusion

1. Velocity profiles show a parabolic in nature. Furthermore, it has an increasing behavior at the center part of the channel with an increase of ϕ, F_0 where the flow is reflected at the walls of the channel. Opposite behavior is noted with the increasing of M, ϵ.
2. Pressure gradient magnitude is an increasing function due to the increase of ϕ, α, Re, while it is a decreasing function with the increase of Fr, M, and it has mixed behavior with the increase of ϵ.
3. In the pumping regions, the pumping rate increases in the retrograde region with an increase of Bn, M, α, Re. The pumping rate increases in the free pumping region with an increase of ϕ, Bn, α, Re. The pumping rate increases in the augmented region with an increase of $\phi, \epsilon, \alpha, Re$.
4. It is noticed that the values of the axial shear stress increase with the increase of M, Bn. While it decreases with the increase of ϕ, F_0.
5. The temperature distribution increases at the central region of the channel with an increase of $\epsilon, F_0, M, Du, Sr, Sc,$ Pr and Br and it decreases with an increase of ϕ and B_{i1}.
6. The profiles of the temperature distribution are parabolic.
7. The Concentration distribution decreases at the central region of the channel with an increase of $\epsilon, F_0, M, Du, Sr, Sc,$ Pr and Br and it increases with an increase of ϕ and x_{i1}.
8. The number and the size of bolus rise up with an increase of ϕ and ϵ. But the converse is seen with an increase of M and Bn.

References

1. Hayat, T., Bibi, S. and Rafiq, M. **2016.** Effect of an inclined magnetic field on peristaltic flow of Williamson fluid in an inclined channel with convective condition. *Journal of magnetism and magnetic materials*, **401**: 733-745.
2. Hayat, T., Shah, S., .Ahmed, B. and Mustafa, M. **2014.** Effect of slip on peristaltic flow of Powell-Eyring fluid in a symmetric channel. *Applied bonics and Biomechanics*, **11**: 69-79.
3. Adel, H. and Abdualhhadi, A. **2017.** The peristaltic transport of MHD Powell- Eyring fluid through porous medium in a symmetric channel with slip condition. *International journal of science and research*, **6**(12).
4. M.Bhatti, M., Zeeshan, A. and Ijaz, N. **2016.** Simultaneous effect of slip and MHD on peristaltic blood flow of Jeffery fluid through porous medium. *Alexandria Engineering Journal*, **55**: 1017-1023.
5. Tanveer, A., Alsaedi, A., Shafique, M. and Hytat, T. **2016.** Magnetohydrodynamic effect on peristaltic flow of hyperbolic tangent nonofluid with slip conditions and joule heating in an inclined channel, *Int. J. Heat and mass. Tran*. **102**: 54-63.
6. Adnan, F.A. and Abdualhadi, A.M. **2019.** Effect of a magnetic field on a peristaltic transport of Bingham plastic fluid in a symmetrical channel. *Sci. int. (Lhore)*.2019. **31**(1): 29-40.
7. Adnan, F.A. and Abdualhadi, A.M. **2018.** Effect of the magnetic field on a peristaltic transport of Bingham plastic fluid. Jour. of adv. *Research and control* .2018. **10**(10).
8. Sh. Ahmad, T. and Abdulhadi, A. **2017.** Effect of a magnetic field on peristaltic flow of Jeffery fluid through a porous medium in a tapered asymmetric channel. *Global Journal of Mathematics*. 2017. **9**(2).